Keyhole Double-Sided Arc Welding Process

A process is developed for deep joint penetration welding in a narrow groove on plate up to ½-in. thick

BY Y. M. ZHANG, S. B. ZHANG, AND M. JIANG

ABSTRACT. Double-sided arcing uses two torches on the opposite sides of the workpiece to force the welding current to flow through the thickness. If a keyhole is established through the thickness, part of the welding current will flow through the keyhole and maintain the electric arc inside the keyhole. It was found the through-thickness direction of the welding current and the establishment of a keyhole both helped enhance the concentration of the arc and the density of the arc energy. In addition, the presence of the arc in the keyhole provided a mechanism to directly heat the workpiece through the thickness, as well as a mechanism to compensate the energy consumed during heating. In this study, a double-sided arcing technique was developed into a welding process for deep, narrow joint penetration. Experiments confirmed the characteristics of this process.

Introduction

Productivity improvement is a major focus for the welding industry and its associated research community, especially in welding of thick materials. Improved methods and processes are required to weld thick materials in a single pass to optimize productivity. Currently the primary processes used for this are electron beam welding and laser beam welding. Both processes require close-tolerance joint fitup and are expensive to operate. Electron beam welding generally requires the use of a vacuum chamber and is, therefore, somewhat limited in application. Laser systems require high capital investment and have high operating and maintenance costs.

High capital investment, maintenance costs, and the positioning and fitup accuracy requirements (Ref. 1) are among the factors that weaken the laser's competitiveness compared to traditional arc welding processes in certain heavy industry applications. However, if the material is not so thick that the reduction in the number of passes is dramatic, the time needed for additional positioning and fitup adjustment due to the high requirement may not justify the high cost. Hence, for such applications, methods or processes that achieve penetration up to ½ in. and that leverage the advantages of conventional arc welding in terms of reduced fitup tolerance, standard operating procedure, personnel, and costs may provide competitive solutions.

One method that improves penetration is to spray a fluxing agent on the workpiece surface during gas tungsten arc welding to modify the flow in the weld pool (Ref. 2). Investigations have focused on experiments for suitable fluxing agents, which are typically mixtures of inorganic powders suspended in a volatile medium, for different materials. This method, referred to as flux-assisted gas tungten arc welding (GTAW), has found successful applications in pipe welding.

Another method to improve penetration in arc welding is to improve the energy density of the arc because energy density is the primary factor responsible for the penetration difference between laser/electron beam welding and arc welding. Research has been done to improve arc concentration by using magnetic means (Refs. 3, 4). However, in addition to the configuration complexity, the effect on arc concentration was found to be limited. Hence, this study explores another method to improve arc concentration and arc energy density to improve penetration with arc welding.

KEY WORDS

Double-Sided Welding
Keyhole
Narrow Joint
Narrow Groove
Deep Penetration
Thick Weldments

Double-Sided Arcing

The proposed arc concentration method relies on a different arcing technique. As can be seen in Fig. 1A, a regular arc welding system uses an electrical connection (workpiece lead) between the workpiece and the power supply to allow the welding current to complete a loop. The electric arc is established between the workpiece and the torch. However, if the workpiece is disconnected from the power supply and a second torch is placed on the opposite side of the workpiece to complete the current loop, as can be seen in Fig. 1B, the electric arc can be simultaneously established between the workpiece and each of the torches, as shown in Fig. 2, where torch one and torch two are for plasma arc welding (PAW) and gas tungsten arc welding (GTAW), respectively. Because the arc is established on both sides of the workpiece, this phenomenon is referred to as double-sided arcing (DSA), and the resultant welding process is referred to as double-sided arc welding (DSAW). Of course, the double-sided arcing phenomenon can be explained by established arc physics. However, it generates certain unique characteristics that are not associated with regular arcing processes.

An obvious characteristic is the direction of the current. Because of the connection between the workpiece and the power supply, the workpiece is an essential element of the current loop in regular arc welding. The current travels in the workpiece at directions approximately parallel to the surface of the workpiece. For example, in keyhole PAW, the majority of the welding current flows from the arc into the surface of the workpiece (Ref. 5). The keyhole is filled with an electrically

Y. M. ZHANG (ymzhang@engr.uky.edu*), S. B. ZHANG, AND M. JIANG are with Welding Research Laboratory, Center for Robotics and Manufacturing Systems and Department of Electrical Engineering, University of Kentucky, Lexington, Ky.*

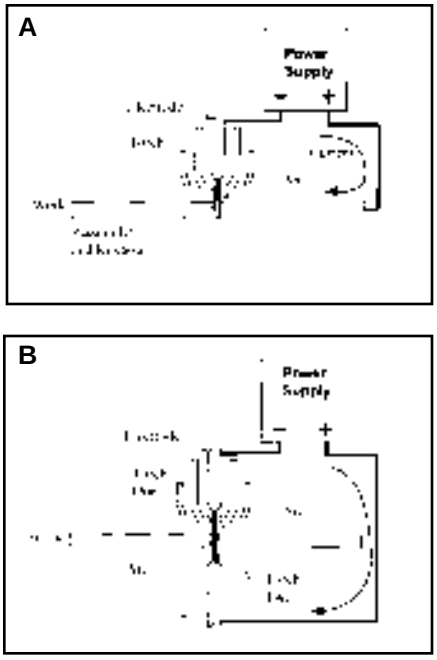

Fig. 1 — Schematic diagrams of welding systems. A — Regular welding system; B — double-sided arc welding system.

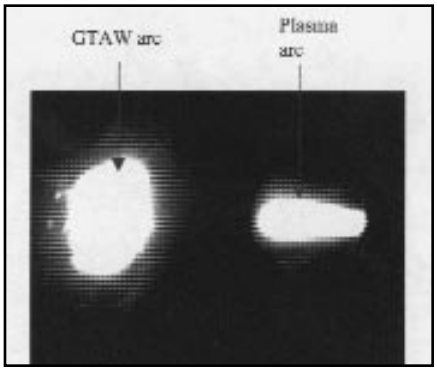

Fig. 2 — Double-sided arcing phenomenon. The workpiece is between the two arcs.

neutral mix of ions and electrons, and the welding current is absent in the keyhole. However, in the double-sided arcing process, the current has to flow through the thickness of the workpiece.

Although the through-thickness direction of the current is associated with different torch combinations (Ref. 6), the specific approach in this study is to use a combination of a PAW torch and a GTAW torch, as shown in Fig. 3, to establish a keyhole through the workpiece. A GTAW/GTAW torch combination has been used to AC weld aluminum in a nonkeyhole mode. (Refs. 7, 8). It is known that the PAW torch has a constricting orifice such that electrons emitted from the tungsten electrode flow through the ionized plasma gas and form a highly constricted plasma jet. This plasma jet melts the workpiece and can displace the molten metal to form a keyhole or deep narrow cavity. Therefore, the PAW/GTAW torch combination may generate the keyhole double-sided arcing phenomenon.

When the keyhole is present, the ionized plasma gas flows from the PAW torch side to the GTAW torch side through the keyhole. Because the ionized plasma gas is an electric conductor, it provides a possible path for the current to flow through the thickness, as shown in Fig. 3. Another possible path of the current is through the metal around the keyhole. For the current to flow through the keyhole, the minimum voltage principle (Ref. 9), i.e., the current takes the path that minimizes the voltage drop, must be satisfied as the necessary condition.

Figure 4 shows the decomposition of the voltage drops for the two paths. If the current takes the metal path, the electrons emitted from the PAW torch's electrode must enter the metal and then re-emit from the bottom surface (the surface of the workpiece on the GTAW torch side). Therefore, the voltage drop will be

$$V = V_{EC} + V_{C1} + V_{WA} + V_{WC} + V_{C2} + V_{EA} \quad (1)$$

where V_{EC} = voltage of electrode cathode; V_{C1} = voltage of arc column one; V_{WA} = voltage of work anode; V_{WC} = voltage of work cathode; V_{C2} = voltage of arc column two; and V_{EA} = voltage of electrode anode. However, if the keyhole is the current path, the voltage drop will be

$$V = V_{EC} + V_{C1} + V_K + V_{C2} + V_{EA} \quad (2)$$

where V_K is the voltage of the keyhole arc column. The minimum voltage principle can only be satisfied if the following condition is met:

$$V_K < V_{WA} + V_{WC} \quad (3)$$

When the thickness of the workpiece, which is approximately the length of the keyhole, is given, the voltage across the keyhole column can be determined as

$$V_K = EL_K \quad (4)$$

where E (V/mm) is the electric field and L_K (mm) is the length of the keyhole column. Although E depends on a number of parameters, it is typically considered a constant when the current and the composition of the shielding gas are given (Ref. 9). For example, if the shielding gas is argon and the current is 200 A, $E \approx$ 0.65 V/mm. Further, if the thickness is ½ in. (12.5 mm), $V_K \approx$ 8V. On the other hand, when the current and the shielding gas are 200 A and argon, respectively, the sum of the cathode and anode voltage drop is approximately 9 V. Hence, for materials ½ in. thick or thinner, the minimum voltage principle can be satisfied. As a result, it becomes possible for the keyhole to become an element of the current loop and for the electric arc to be present in the keyhole if the thickness is not greater than ½ in.

Arc Concentration and Energy Compensation

Figures 5 and 6 show the arc behaviors for regular PAW and DSAW before and after the keyhole is established. Two phenomena can be observed from these figures. First, in comparison with regular plasma arc, the plasma arc in DSAW becomes much more concentrated despite the use of similar welding parameters. Second, after the keyhole is established, the plasma arc in DSAW is further concentrated while the regular plasma arc remains unchanged.

During DSAW, current has to flow from one torch to another through the workpiece, or the keyhole, as illustrated in Fig. 4. If the current flows through the workpiece instead of the keyhole, the elec-

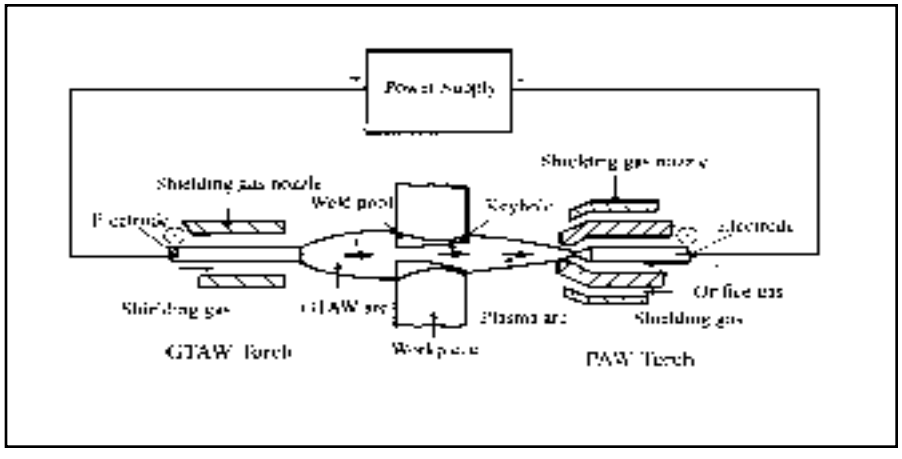

Fig. 3 — Proposed welding system for keyhole DSAW.

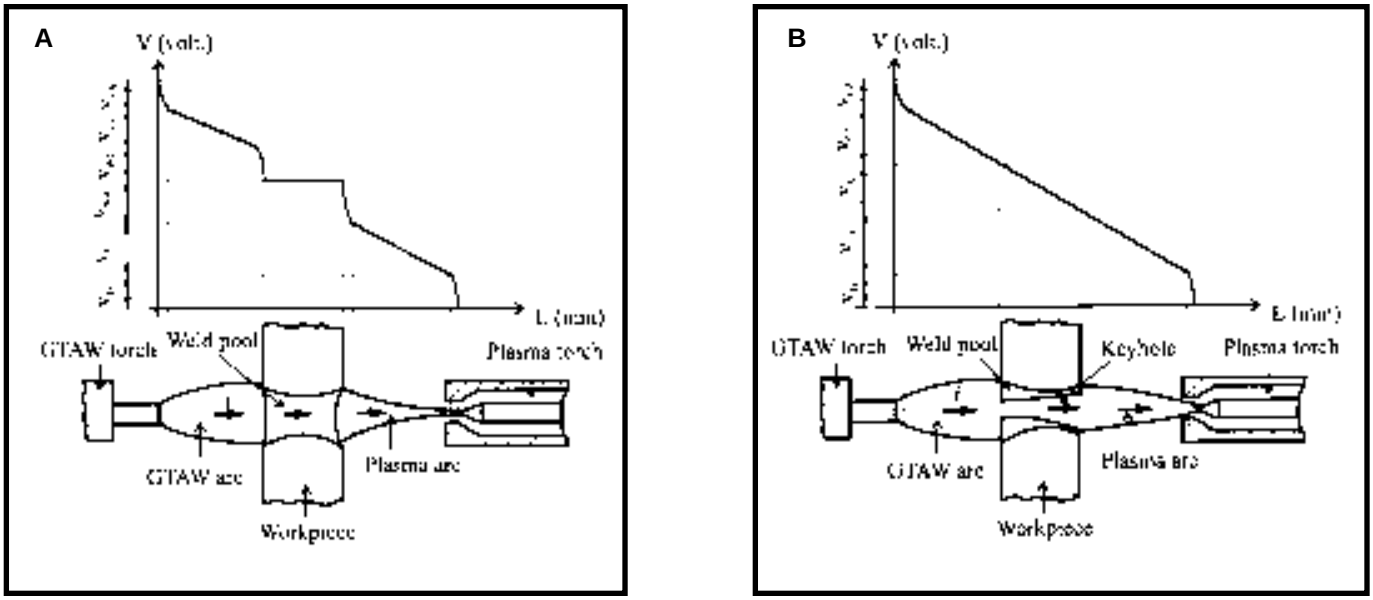

Fig. 4 — Voltage decomposition in DSAW. A — Nonkeyhole mode; B — keyhole mode.

trons must exit from the workpiece through the cathode on the GTAW side surface of the workpiece to the GTAW electrode. Because of the large current needed for welding, the electrons tend to emit from the workpiece from an area rather than a small spot. Hence, the workpiece cathode is typically much less focused than the anode (Ref. 9). As a result, the GTAW arc in DSAW is much broader than the plasma arc.

Assume the radius of the workpiece cathode is 3 mm and the thickness of the workpiece is 10 mm. The radius of the plasma jet is approximately 1 mm. That is, the radius of the current flow increases by 2 mm through a 10-mm distance. The average diffusion angle of the current in the workpiece is thus $\alpha = \text{Tan}^{-1}\, 0.2 \approx 10$ deg. Because this diffusion angle is so small, the electrons can easily realize their transition in direction when they enter the workpiece from the plasma arc column. The trajectory of the electrons (current) in the plasma arc column is not affected by the workpiece. However, for regular PAW, the electrons have a nearly 90-deg transition in direction when they enter the workpiece. To realize such a large transition in travel direction, the electrons must change their direction prior to "landing" on the workpiece. The arc column in regular plasma arc welding, thus, must be subject to a divergence. Hence, the plasma arc in DSAW is much more concentrated than the regular plasma arc, as seen in Figs. 5A and 6A.

The establishment of the keyhole further enhances the concentration of the plasma arc in DSAW. After the keyhole is established, the current may take the keyhole as the path. In this case, the current

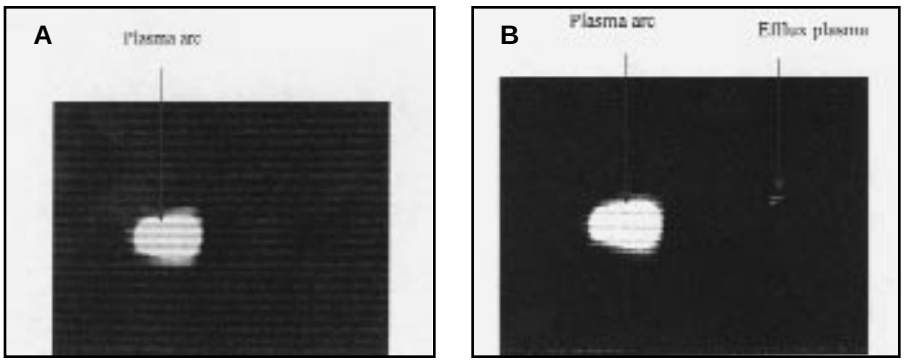

Fig. 5 — Arc behaviors before and after the keyhole is established during regular PAW. The efflux plasma indicates the establishment of the keyhole. Welding current: 120 A, diameter of the orifice: 2.4 mm, flow rate of the orifice gas (argon): 1.8 L/min. A — Before; B — after.

flows through the keyhole without being affected by the workpiece cathode, the diameter of which is much larger than that of the keyhole. The plasma arc can thus be further concentrated. As can be seen, the diameter of the plasma arc in Fig. 6B is less than 70% of that in Fig. 6A. Hence, the density of the plasma arc is at least doubled after the keyhole is established.

As can be seen in Fig. 6B, the GTAW arc is still broad after the keyhole is established. This indicates that, although the electrons can flow through the keyhole to minimize the voltage, part of them actually flow through the workpiece, causing a cathode on the workpiece. Therefore, during keyhole DSAW, only part of the current goes through the keyhole. The rest of the current flows through the workpiece.

An interesting question is why part of the current goes through the workpiece instead of the keyhole, which minimizes the voltage. Although detailed studies, which are beyond the scope of this paper and which first introduced keyhole DSAW, are needed to answer this fundamental question, the authors suspect the high-speed impact of the electrons on the workpiece may be the factor responsible. In fact, part of the electrons may hit the workpiece when they are traveling along the keyhole, which is not perfectly straight. Because of the high speed of the electrons in the highly constricted plasma jet, the electrons have sufficient energy to enter the workpiece.

Another interesting question is what percent of current flows through the workpiece, rather than through the keyhole, after the keyhole is established. It is understandable that an accurate estimate of this percentage is difficult because it may depend on many parameters, such as the

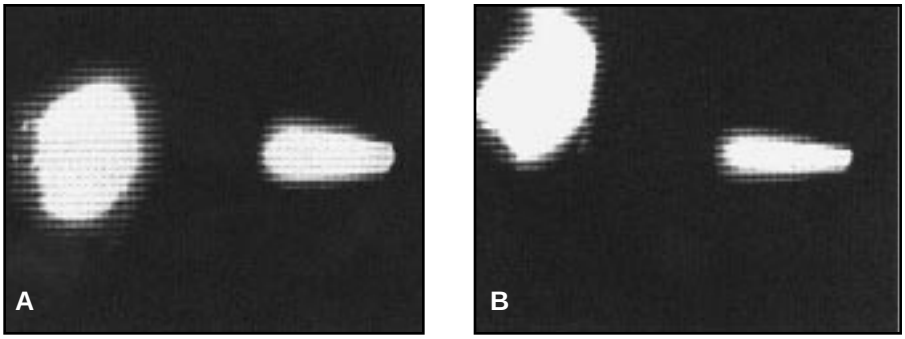

Fig. 6 — Arc behaviors before and after the keyhole is established during DSAW. Welding current: 120 A, diameter of the orifice: 2.4 mm, flow rate of the orifice gas (argon): 1.8 L/min. A — Before; B — after.

shape of the keyhole, the diameter of the orifice, the flow rate of the orifice gas, and the speed of the electrons, etc. However, experimental results in Fig. 6 give us an approximate estimate. In Fig. 6, the density of the arc, or current, is doubled after the keyhole is established. If we assume this concentration in the current flow is caused by the establishment of the keyhole, one may estimate at least 50% of the current flows through the keyhole.

To verify the accuracy of the above estimate, the voltage signal when the process changes from keyhole to nonkeyhole mode is recorded for keyhole DSAW, as seen in Fig. 7. In the experiment, the thickness of the workpiece is 6.4 mm. The ratio of the current p flowing through the keyhole can be estimated by using the following equation:

$$\Delta V = (V_{WC} + V_{WA}) - \{V_K p + (V_{WC} + V_{WA})(1 - p)\} = (V_{WC} + V_{WA} - V_K)p \quad (5)$$

where ΔV is the voltage decrease from nonkeyhole to keyhole mode, which is approximately 3.5 V; V_K is the voltage drop of the keyhole column, which is approximately 4 V when the thickness is 6.4 mm; $V_{WC} + V_{WA}$ is the voltage drop if the current fully flows through the workpiece; and the weighted sum $V_K p + (V_{WC} + V_{WA})(1 - p)$ is used as an estimate of the average voltage of the keyhole and the workpiece. Equation 5 gives

$$p = \frac{\Delta V}{V_{WC} + V_{WA} - V_K} = \frac{3.5}{10 - 4} = 0.58 \quad (6)$$

Hence, analysis of the voltage decrease suggests that more than 50% of the current flows through the keyhole. This is similar to the estimation made based on the arc concentration.

It should be pointed out that, with regard to the estimate for arc concentration after the establishment of the keyhole, the voltage decrease associated with the establishment of the keyhole is only observed during DSAW, not during regular PAW. Figure 8 plots the voltage signal during nonkeyhole and keyhole mode for regular PAW. No difference in the voltage signal can be found. Of course, it is understandable because the majority of the current during regular plasma arc welding is "earthed" through the surface of the workpiece (Ref. 5). The establishment of the keyhole plays no noticeable role in changing the arc behavior (current flow distribution) and the voltage.

In addition to the arc concentration as analyzed above, another unique characteristic associated with DSAW — energy compensation along the thickness — is caused by the presence of the arc in the keyhole. That is, in regular keyhole PAW, the current does not flow through the keyhole (Ref. 5). The ionized gas jet thus loses its initial energy, gained before it enters into the keyhole from the arc, to heat the wall of the keyhole without energy compensation. However, in the keyhole DSAW process, the current flowing in the ionized gas jet generates the arc in the keyhole. As a result, the energy consumed to heat the wall of the keyhole can be at least partially compensated. For ⅜-in.- (9.5-mm-) thick material, $V_K \approx$ 6 V, which is approximately ½ of the welding voltage, and the compensated arc energy is approximately ½ of the total arc energy. More importantly, this part of energy directly heats the workpiece through the thickness direction radially. Its contribution to the penetration is thus much more effective than the arc energy in other parts of the arc. Hence, although an accurate estimate of its contribution to penetration improvement requires detailed studies beyond the scope of this introductory work, it is certain this contribution is quite significant.

Experiments and Results

The keyhole double-sided arcing technique may be used to develop an effective keyhole DSAW process to achieve narrow, deep penetration. To this end, an experimental setup, shown in Fig. 3, was developed. It uses a DC constant-current power source. This DC power supply is capable of providing a constant current from 50 to 200 A with voltage up to 50 V. A regular PAW torch and a GTAW torch are connected to the negative terminal and positive terminal of the power supply, respectively.

Table 1 — Invariant Welding Parameters

Orifice diameter	1.57 mm (0.062 in.)
Electrode diameter: PAW torch	4.8 mm (3/16 in.)
Electrode diameter: GTAW torch	4.8 mm (3/16 in.)
Flow rate of orifice gas	1.15 L/min (2.5 ft³/h)
Flow rate of shielding gas (plasma torch)	13.8 L/min (30 ft³/h)
Flow rate of shielding gas (GTAW torch)	23 L/min (50 ft³/h)
Standoff (PAW electrode)	6 mm (0.24 in.)
Standoff (GTAW electrode)	10 mm (0.38 in.)

Table 2 — Variable Welding Parameters

Sample No.	Process	Thickness (mm)	Type of Joint	Root Opening	Filler Metal Use	Welding Voltage (V)	Welding Current (A)	Travel Speed (mm/min)	Welding Position
1	PAW	6.4	Sq. Butt	Zero	None	30	70	40	Flat
2	DSAW	9.5	Sq. Butt	Zero	None	45	70	80	Flat
3	DSAW	12.7	Sq. Butt	Zero	None	45	70	50	Uphill

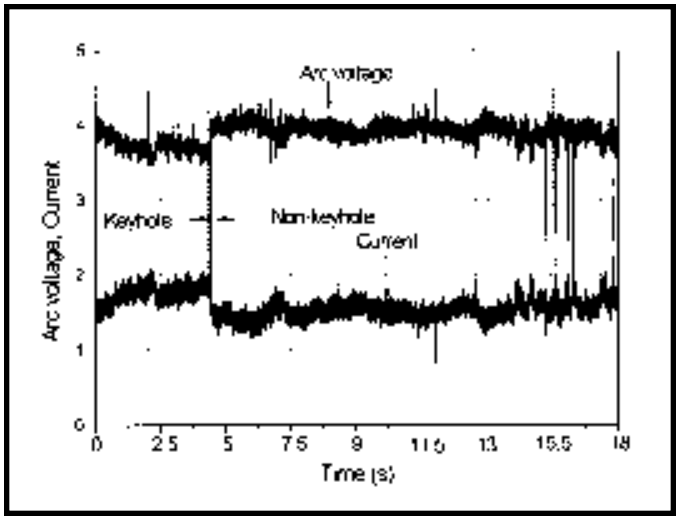

Fig. 7 — Voltage signal in keyhole and nonkeyhole mode during DSAW.

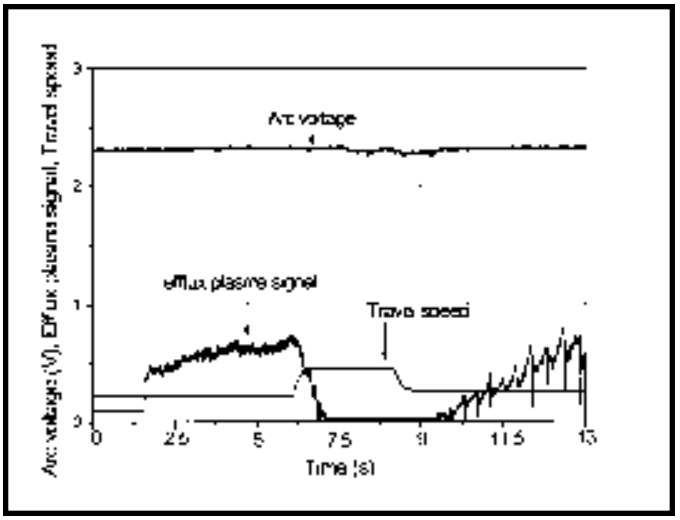

Fig. 8 — Voltage signal in keyhole and nonkeyhole mode during regular PAW. The efflux plasma signal indicates the establishment of the keyhole.

The austenitic stainless steel used in the experiments is commercial plate Type 304 (wt-% 0.08 C, 2.00 Mn, 1.0 Si, 18.0-20.0 Cr, 8.0–10.5 Ni, 0.045 P, 0.03 S and Bal. Fe). Since keyhole PAW achieves deeper penetration than all existing arc welding processes, comparison will be made between PAW and DASW. Because of the improved arc concentration, DSAW is capable of penetrating 12.7 mm (½ in.) in a single pass. On the other hand, it is not easy to keyhole plasma arc weld stainless or other steel plates as thick as 9.7 mm (⅜ in.) in a single pass without producing a gap (Ref. 10). Hence, 6.4-mm- (¼-in.-) thick plate was welded using keyhole PAW, and 9.5-mm- (⅜ -in.-) and 12.7-mm- (½ -in.-) thick plates were welded using keyhole DSAW, respectively, for comparison.

Because no previous data is available, experiments have been done to determine the welding parameters for keyhole DSAW. The criterion is that the selected welding parameters produce the desired full penetration without melt-through. Because of the impact of the plasma, underfill typically results in the plasma arc side. However, desired reinforcement can be easily achieved by a standard follow-up cover pass. To ease the comparison, filler metal is not used in this study for both PAW and DSAW. Tables 1 and 2 list the experimentally determined welding parameters.

Narrow, Deep Joint Penetration

Figure 9 shows a keyhole double-sided arc weld, Sample 2 in Table 2, on 9.7-mm- (⅜-in.-) thick stainless steel plate. The welding speed was 80 mm/min. The width of the weld zone in the middle portion along the thickness direction remains below 2.5 mm. For the same thickness, a 10-kW laser beam achieves full penetration with a narrower weld of 2 mm (Ref. 1). Of course, the speeds achieved with lasers are much faster.

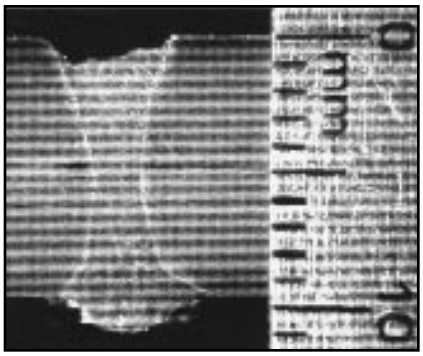

Fig. 9 — Keyhole double-sided arc butt joint weld on 9.5-mm (⅜-in.) plate (Sample 2). Position: flat, welding current: 70 A, travel speed: 80 mm/min, filler metal: none.

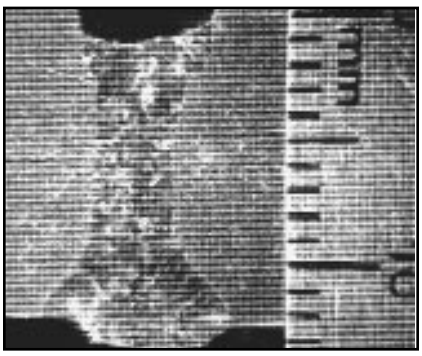

Fig. 10 — Keyhole double-sided arc butt weld on 12.7-mm (½-in.) plate (Sample 3). Position: uphill, welding current: 70 A, travel speed: 50 mm/min, filler metal: none.

Figure 10 gives a keyhole double-sided arc weld (Sample 3 in Table 2) on 12.7-mm- (½-in.-) thick stainless steel plate. The welding speed was 50 mm/min. The width of the weld zone in the middle portion along the thickness direction remains below 3.5 mm. For the same thickness, a 9.1-kW laser beam achieves full penetration at the width of 3 mm (Ref. 11).

It can be seen that deep, narrow penetration has been achieved by the keyhole DSAW process. Such deep penetration significantly reduces the weld pool and makes it possible to weld thicker materials in a single pass without melt-through. For example, in typical applications, ½-in.-thick steel plates require machined bevels and five to six passes (Ref. 12). As can be seen, keyhole DSAW achieved full penetration without bevel in a single pass. The resultant productivity improvement and filler metal reduction are substantial.

Heat Input

The power of an arc can be calculated as

$$P_{arc} = IV \qquad (7)$$

Where I and V are the welding current and welding voltage, respectively. However, the actual heat input into the workpiece is not exactly given by the power of the arc.

For regular PAW, the voltage can be decomposed into

$$V = V_{EC} + V_C + V_{WA} \qquad (8)$$

where V_{EC} = voltage of the electrode cathode, V_C = voltage of the plasma arc column, and V_{WA} = the voltage of the workpiece anode. Among the three voltage components, V_{EC}, V_C, and V_{WA}, the heat input into the workpiece is primarily determined by the latter two. Therefore, the effective power of the arc, which will be converted as the workpiece heat input during keyhole PAW, can be expressed as

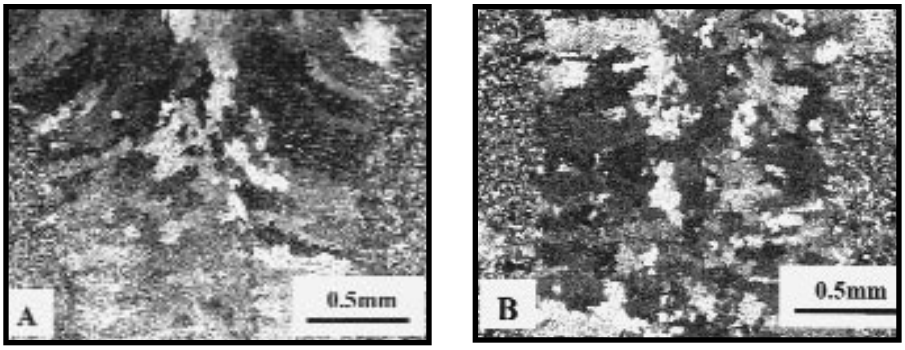

Fig. 11 — Solidification structures of the weld metal zones. A — Sample 1: PAW, 6.4 mm, butt joint, no filler metal; B — Sample 2: DSAW, 9.5 mm, butt joint, no filler metal.

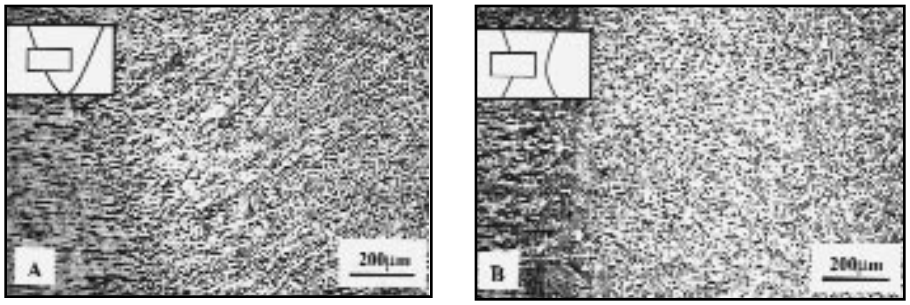

Fig. 12 — Micrographs around the weld boundaries. A — Sample 1: PAW, 6.4 mm, butt joint, no filler metal; B — Sample 3: DSAW, 12.7 mm, butt joint, no filler metal.

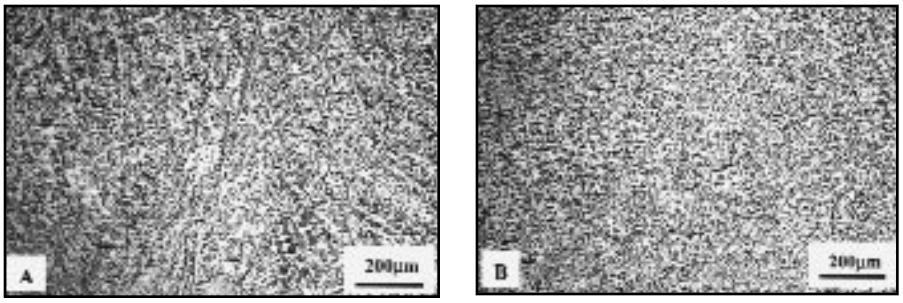

Fig. 13 — Micrographs in the center of the weld boundaries. A — Sample 1: PAW, 6.4 mm, butt joint, no filler metal; B — Sample 3: DSAW, 12.7 mm, butt joint, no filler metal.

$$P_{e,r} = \eta I(V_C + V_{WA}) = \eta I(V - V_{EC}) \quad (9)$$

where $\eta < 1$ is a constant, which accounts for the heat loss of the arc due to radiation, and is referred to as the arc efficiency.

For keyhole DSAW, the parts of the welding current flowing through the keyhole and the metal surrounding the keyhole are pI and $(1 - p)I$, respectively. For the convenience of discussion, assume the arc consists of two parallel arcs corresponding to the two parts of the current. For both arcs, the anode and cathode voltage on both tungsten electrodes should be removed from the total voltage during computing the effective power. This implies the effective power during keyhole DSAW can be estimated as

$$P_{e,d} = \eta_1 pI\,(V_{C1} + V_K + V_{C2}) + \eta_2(1-p)I(V_{C1} + V_{WA} + V_{WC} + V_{C2}) = \eta_1 pI(V_1 - V_{EC} - V_{EA}) + \eta_2(1-p)I(V_2 - V_{EC} - V_{EA}) \quad (10)$$

where V_1 is the voltage of the arc corresponding to the part of the current flowing through the keyhole, and V_2 is the voltage of the arc corresponding to the part of the current flowing through the metal surrounding the keyhole, and constants $\eta_1 < 1$ and $\eta_2 < 1$ are their efficiency. Because the heat generated by the cathode and anode spots is almost totally put into the workpiece, the arc efficiency for three arc columns is not higher than that for two arc columns and a anode and cathode pair, i.e., $\eta_1 \leq \eta_2$. When $p = 0.5$,

$$P_{e,d} \leq 0.5\eta_2 I(V_1 - V_{EC} - V_{EA} + V_2 - V_{EC} - V_{EA}) = \eta_2 I\{0.5(V_1 + V_2) - V_{EC} - V_{EA})\} = \eta_2 I(V - V_{EC} - V_{EA}) \quad (11)$$

where V is the average voltage measured. Further, because $V_{WA} >> V_{WC}$, the arc efficiency for two arc columns and an anode and cathode pair is not higher than that for one arc column and an anode. That is, $\eta_2 \leq \eta$. As a result,

$$P_{e,d} \leq \eta I(V - V_{EC} - V_{EA}) \quad (12)$$

Equations 9 and 12 provide a way to estimate the heat input into the workpiece for the welded samples in the experiments. In the first comparison, the ratio of heat input of the keyhole DSAW to the regular keyhole PAW is computed. As seen below, the computed ratio of heat input between these two processes is independent of the arc efficiency in Equations 9 and 12. Hence, in the following discussion, a typical value 0.7 is assumed for the arc efficiency. Hence, for Samples 2 and 3 where current and voltage are 70 A and 40 V

$$P_{e,d} \leq \eta 70(45 - V_{EC} - V_{EA}) \approx 0.7 \text{ x } 70(45 - 9) = 1764 \text{ W} \quad (13)$$

For Sample 1 (¼ in. thick),

$$P_{e,r} = hI(V - V_{EC}) = \eta 70(30 - V_{EC}) \approx 0.7 \text{ x } 70(30 - 2) = 1372 \text{ W} \quad (14)$$

To penetrate ¼-in.-thick plate, regular keyhole PAW uses a 1372-W effective heat source at the travel speed of 40 mm/min. For keyhole DSAW, ⅜-in.-thick plate can be penetrated using a 1764-W effective heat source at the travel speed of 80 mm/min. The heat input of keyhole DSAW for ⅜-in.-thick plate is thus only approximately 60% the heat input of regular keyhole PAW for ¼-in.-thick plate. If keyhole PAW is used to penetrate ⅜-in.-thick plate, the heat input would be at least double the heat input used for ¼-in. plate. Hence, the heat input required to weld ⅜-in.-thick plate by keyhole DSAW is at most 30% of that needed by keyhole PAW.

The heat input comparison can also be made between DSAW and laser beam welding. For 9.5-mm- (⅜-in.-) thick plate, a 10-kW laser beam can achieve full penetration at the travel speed of 80 in./min, or 2032 mm/min (Ref. 1). The heat input is thus approximately 20% as the heat input of keyhole DSAW. For 12.7-mm- (½-in.-) thick plate, a 9.1-kW laser beam achieves the full penetration at the travel speed 900 mm/min. The heat input into the workpiece is again approximately 20% of the heat input associated with keyhole DSAW for the same thickness.

Weld Shape

As can be seen in Figs. 9 and 10, the cross sections of double-sided arc welds are approximately symmetrical and hourglass shaped. Although detailed studies are needed to determine the effectiveness of this shape in thermal distortion and residual stress reduction, it is certain the thermal distortion and residual stress must be reduced.

Grain Structure

Specimens cut from the weld samples are mechanically polished and chemically etched with a solution of 340 g $FeCl_3 \cdot 6H_2O$ + 125mL HCl + 40 mL HNO_3 + 250 mL H_2O to reveal the macrostructure and electrolytically etched with a solution of 10 g oxalic acid + 100 mL water to determine the microstructure. The macrostructures are examined using a Nikon SMZ800 stereoscopic zoom microscope. The microstructures are observed by using a Nikon Epiphot 300 optical metallurgical microscope and a Hitachi S-3200 scanning electron microscope (SEM), operated at 20 kV.

Figure 11 shows the morphologies of solidification macrostructures in the welded joint in comparison with keyhole PAW joints. Figure 12 shows the microstructures around the weld boundary, and Fig. 13 shows the microstructures in the center of the weld metal zone. Compared to regular plasma arc welded joint (Figs. 11A, 12A, and 13A), fine equiaxed solidification grains were formed in the bulk of the weld metal zone of DSAW, with only a very narrow columnar region along the weld boundary, as shown in Figs. 11B, 12B, and 13B.

Generally, the solidification structure is controlled by the solidification parameters — the solidification growth rate R and the thermal gradient in the liquid G_L. The ratio of the two parameters G_L/R normally changes from a maximum value at the fusion boundary to a minimum along the center of the weld. These changing solidification conditions result in a weld solidification structure changing from planar at the weld boundary to columnar dendrite and then to equiaxed dendrite grain along the weld center (Ref. 13). For DSAW process, it was found the fraction and width of the fine equiaxed grain region gradually increases in the weld metal zone along with an increase in the depth of penetration. It is known that when the penetration increases, the amount of molten metal increases. Such an increase in the amount of molten material helps heat the workpiece before cooling; hence, the thermal gradient during cooling is reduced. This tends to allow an increase in the amount of fine equiaxed grains produced.

Conclusions

Double-sided arcing phenomenon and technique have been used to develop the keyhole DSAW process. Observation and analysis show the through-thickness direction of the current and the establishment of the keyhole both play significant roles in enhancing arc concentration.

Experimental data and analysis suggest at least part of the current flows through the keyhole if the keyhole provides a minimum voltage path. The presence of the current in the keyhole generates an energy compensation not found in other arc welding processes.

The keyhole DSAW process has proven capable of achieving deep, narrow joint penetration on square-groove, thick stainless steel plates up to ½-in. in a single pass.

Keyhole DSAW reduces heat input into the workpiece by at least 70% in comparison with regular keyhole PAW, which achieves the deepest and narrowest penetration at the least heat input of all existing arc welding processes. In other words, keyhole DSAW requires only 30% of the heat input needed by keyhole PAW.

Welds produced by keyhole DSAW are less than 1 mm wider than those produced by the laser process. To penetrate the same thickness of stainless steel plates up to ½ in. thick, the heat input into the workpiece by the keyhole DSAW process is approximately five times as much as that input by a high-power (approximately 10-kW) laser.

Welds produced by keyhole DSAW are approximately symmetrical and hourglass shaped.

Keyhole DSAW tends to increase the amount of the desirable equiaxed grains in the solidified welds.

Detailed studies are needed to fully disclose the metallurgical implications and mechanical properties for keyhole DSAW of different materials, including the impact of heat input reduction and symmetrical shape on thermal distortion and residual stress, and to quantitatively analyze the phenomena during double-sided arcing and the keyhole double-sided arc welding process.

Acknowledgments

This work was funded by the National Science Foundation under Grant DMI-98 12981 and the Center for Robotics and Manufacturing Systems at the University of Kentucky. The authors would also like to thank The Lincoln Electric Company, Thermal Arc, Inc., and NASA Marshall Space Flight Center for financial, equipment, and material support. Finally, the authors wish to thank the late Warren Mayott at The Electric Boat and Dr. Arthur Nunes at Marshall Space Flight Center for fruitful technical discussions.

References

1. *Welding Handbook*. 8th edition, Vol. 2, Welding Processes. Miami, Fla.: American Welding Society.

2. McGaughy, T. 2000. Two new technologies may increase pipe production and reduce cost. *Welding Journal* 70(8): 65–66.

3. Welz, W. 1990. Magnetically impelled arc pressure welding of non-magnetic steels. *Schweissen und Schneiden*, 42(2): 24–26.

4. Satoh, T., Katayama, J., Ioka, S., and Otani, M. 1990. Experimental study on rotating behavior of arc during magnetically impelled arc butt welding. *Quarterly Journal of the Japanese Welding Society* 8(1): 71–77.

5. Dowden, J., and Kapadia, P. 1994. Plasma arc welding: a mathematical model of the arc. *Journal of Physics (D): Applied Physics* 27: 902–910.

6. Zhang, Y. M., and Zhang, S. B. 1999. Method of arc welding using dual serial opposed torches. U.S. Patent, No. 5,990,446.

7. Zhang, Y. M., and Zhang, S. B. 1999. Welding aluminum Alloy 6061 with opposing dual torch GTAW process. *Welding Journal* 78(6): 202-s to 206-s.

8. Zhang, Y. M., Pan, C. X., and Male, A. T. 2000. Improvement of microstructures and properties of 6061 aluminum alloy weldments using double-sided arc welding process. *Metallurgical Transactions A* 31(10): 2537–2543.

9. Lancaster, J. F. 1986. *The Physics of Welding.* Oxford, Pergamon Press.

10. Halmoy, E., Fostervoll, H., and Ramsland, A. 1994. New applications of plasma keyhole welding. *Welding in the World* 34: 285–291.

11. Dawes, C. 1992. *Laser Welding: a Practical Guide*, Cambridge, England: Abington Publishing.

12. Welding Workbook. 2000. Downhill welding of pipe. *Welding Journal* 79(8): 67–68.

13. Puchaicela, J. 1998. Control of distortion of welded steel structures. *Welding Journal* 77(8): 49–52.